ORGANIC CHEMISTRY FRONTIERS

RESEARCH ARTICLE

View Article Online
View Journal | View Issue

Cite this: *Org. Chem. Front.*, 2026, **13**, 2143

Pd(II)-catalyzed intramolecular diarylation of alkynes *via* dual C–H activation: modular access to azafulvalene-based bis(polycyclic) aromatic enes

Tienan Jin, *[b] Sho Aida,[a] Takuma Sato[a] and Masahiro Terada [a]

Bis(polycyclic) aromatic enes (BPAEs), comprising two polyaromatic units bridged by an ethylenic linker, exhibit distinctive electronic properties, yet heteroatom-containing analogues like azafulvalenes remain scarcely explored despite their tunable π-conjugation and redox versatility. Herein, we report an efficient Pd(II)-catalyzed intramolecular diarylation of alkynes that enables the selective synthesis of previously inaccessible azafulvalene-based BPAEs through dual C–H bond activation. This strategy adopts *N*-aryl and 2-aryl-substituted biarylalkynyl indole scaffolds, enabling modular access to structurally diverse azafulvalene-based BPAEs with precisely incorporated nitrogen atoms. Mechanistic investigations and DFT calculations revealed a pivalate-assisted concerted metallation–deprotonation (CMD) pathway, with the syn-insertion step as the rate-determining process. The addition of trifluoroacetic acid significantly lowers the activation barrier of this key step, enhancing the overall reaction efficiency. The synthesized azafulvalene-based BPAEs exhibit broad and red-shifted absorption bands extending up to 650 nm, low-lying LUMO levels (−3.47 to −3.63 eV), and narrow HOMO–LUMO gaps, consistent with donor–acceptor electronic structures predicted by DFT and TD-DFT calculations. This work establishes a modular and atom-economical synthetic approach for constructing π-extended nitrogen-containing fulvalene frameworks and highlights the potential of azafulvalene-based BPAEs as promising building blocks for advanced organic optoelectronic materials.

Received 14th December 2025,
Accepted 11th February 2026

DOI: 10.1039/d5qo01688f

rsc.li/frontiers-organic

Introduction

Bis(polycyclic) aromatic enes (BPAEs) represent a distinctive class of π-conjugated organic molecules in which two polyaromatic units are directly linked by an ethylenic (C=C) bridge. Their rigid and planar π-backbones combined with inherently twisted alkene moieties impart unique electronic, optical, and structural properties, making them attractive candidates for functional organic materials.[1–19] Among these, fulvalene-based BPAEs such as 9,9′-bifluorenylidene (99′BF) and its π-extended analogues have been extensively investigated due to their high electron affinity and strong electron-accepting ability, enabling applications in organic photovoltaics and electronic devices (Scheme 1a).[1–6] The twisted alkene geometry and electronically diverse π-systems of such compounds also support dynamic properties, including molecular switching and oligoradicaloid behavior.[5–12]

In contrast, BPAEs incorporating heterofulvalene units, where one or both rings contain heteroatoms such as nitrogen, oxygen, or sulfur, have received far less attention.[13,14] Tetrathiafulvalene-derived BPAEs are known for their excellent electron-donating character and wide use in advanced electronic materials, while six-membered heterofulvalene analogues such as dihydroacridine, xanthene, and thioxanthene derivatives exhibit unique photoresponsive and redox-active behaviors (Scheme 1a).[15–20] Particularly intriguing are azafulvalene-based BPAEs, in which nitrogen atoms are embedded within the fulvalene core. This underexplored subclass offers promising features such as extended π-conjugation, enhanced electron-donating ability, and tunable redox properties. When combined with electron-deficient fluorenylidene units, azafulvalene frameworks could enable novel optoelectronic functionalities. However, despite the success of conventional synthetic methods, including Barton–Kellogg olefination[1] and transition-metal-catalyzed cyclization,[21–26] no general approach has been established for constructing azafulvalene-based BPAEs.

Transition-metal-catalyzed diarylation of alkynes has recently emerged as a powerful tool for building multifunctionalized alkenes and complex polycyclic frameworks.[22,27–39] In particular,

[a]*Department of Chemistry, Graduate School of Science, Tohoku University, Sendai 980-8578, Japan*
[b]*Research and Analytical Center for Giant Molecules, Graduate School of Science, Tohoku University, Sendai 980-8578, Japan. E-mail: tetsuo.kin.a6@tohoku.ac.jp*

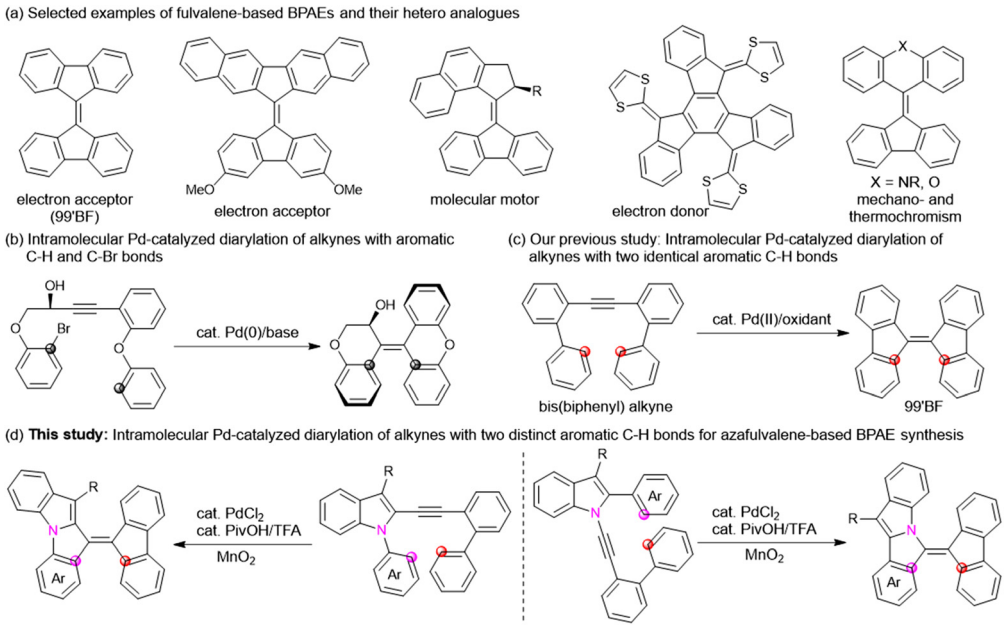

Scheme 1 Pd-Catalyzed diarylation of alkynes *via* C–H activation for synthesis of bis(polycyclic) aromatic enes (BPAEs).

palladium-catalyzed intramolecular diarylation, often involving C–H bond activation, offers an efficient and atom-economical route to π-extended bispolycyclic enes. For example, Pd(0)-catalyzed intramolecular diarylation of diaryl-tethered alkynes bearing C–Br and C–H functionalities efficiently furnishes BPAE skeletons (Scheme 1b).[36–39] More recently, a Pd(II)-catalyzed dual C–H activation of bis(biaryl) alkynes has enabled the direct synthesis of 99′BF-type frameworks without halide prefunctionalization (Scheme 1c).[22] These strategies exemplify the increasing importance of multiple C–H activation as a step- and atom-economical method for building complex π-extended scaffolds. Despite these advancements, the development of modular and general synthetic methods for structurally diverse BPAEs, especially heteroatom-containing variants, remains a synthetic challenge.

Building on these advances, we report a Pd(II)-catalyzed intramolecular diarylation of alkynes that accomplishes selective activation of two distinct aromatic C–H bonds in *N*-aryl- and 2-aryl-substituted biarylalkynyl indole scaffolds (Scheme 1d). This strategy delivers the first general and modular access to azafulvalene-based BPAEs with controlled nitrogen arom incorporation. The resulting π-extended molecules display low-lying LUMO levels, narrow bandgaps, and long-wavelength absorption, underscoring their promise as next-generation organic optoelectronic materials.

Results and discussion

To develop new synthetic methods for azafulvalene-based BPAEs, we examined catalyst systems based on our previous alkyne diarylation strategy (Scheme 1c).[22] Diarylation of 2-alkynyl indole **1a**, bearing an electron-donating *p*-tolyl substituent on the nitrogen atom, proceeded smoothly with a 1 : 1 mixture of $PdCl_2$ and PivOH as catalyst and MnO_2 as oxidant at 80 °C for 6 h, delivering product **2a** in 83% yield (Table 1, entry 1). Altering the

Table 1 Screening of reaction conditions for the reaction of **1a** to **2a**[a]

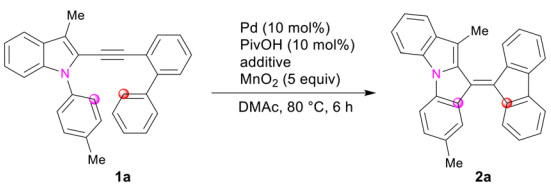

Entry	Cat. Pd(II)	Additive (mol%)	**2a**[b] (%)	**1a**[b] (%)
1	$PdCl_2$		83, 63,[c] 71[d]	9, 22,[c] 20[d]
2[e]	$PdCl_2$		trace	99
3	$PdBr_2$		16	78
4	PdI_2		2	98
5	$PdCl_2(MeCN)_2$		56	40
6	$PdCl_2(PPh_3)_2$		48	40
7	$Pd(OAc)_2$		trace	99
8	$Pd(OPiv)_2$		trace	99
9	$Pd(TFA)_2$		20	80
10	$PdCl_2$	TFA (10)	88	11
11	$PdCl_2$	TFA (20)	96 (94)	0
12[e]	$PdCl_2$	TFA (10)	16	84
13	$PdCl_2$	AcOH (10)	90	4
14	$PdCl_2$	CH_3SO_3H (10)	85	9
15	$PdCl_2$	CsOPiv (100)	0	89

[a] Conditions: **1a** (0.1 mmol), Pd (10 mol%), PivOH (10 mol%), additive (10 mol%), and MnO_2 (5 equiv.) in DMAc (0.125 M, 0.8 mL) at 80 °C for 6 h. [b] ^1H NMR yield determined using CH_2Br_2 as an internal standard. Isolated yield is shown in parentheses. [c] Using 15 mol% of PivOH. [d] Using 5 mol% of PivOH. [e] In the absence of PivOH.

$PdCl_2$: PivOH ratio to 1 : 1.5 or 2 : 1 under otherwise identical conditions lowered yields to 63% and 71%, respectively, indicating an optimal 1 : 1 ratio. No reaction occurred in the absence of PivOH (entry 2), with **1a** recovered nearly quantitatively, demonstrating that PivOH is essential for the C–H activation step. Other Pd(II) halide salts, $PdBr_2$ and PdI_2, showed poor catalytic activity (entries 3 and 4). $PdCl_2$ complexes bearing ligands, $PdCl_2(CH_3CN)_2$ and $PdCl_2(PPh_3)_2$, afforded **2a** in moderate yields (entries 5 and 6). $Pd(OAc)_2$ and $Pd(OPiv)_2$ were completely ineffective, while $Pd(TFA)_2$ gave **2a** in 20% yield (entries 7–9). These comparisons highlight the unique effectiveness of the $PdCl_2$/PivOH combination. Addition of trifluoroacetic acid (TFA) further improved the yield of **2a** to 88% with 10 mol% TFA and 96% with 20 mol% TFA (entries 10 and 11). However, the $PdCl_2$/TFA system without PivOH gave only a low yield of 16% (entry 12), confirming that both PivOH and TFA contribute positively but are not interchangeable. Other Brønsted acids such as AcOH and $MeSO_3H$ also increased conversion (entries 13 and 14). In contrast, the presence of base (CsOPiv) completely suppressed diarylation (entry 15). Finally, replacing MnO_2 with alternative oxidants (2 equiv.), such as AgOPiv (0%), Ag_2O (5%), $CuCl_2$ (0%), or CuO (5%), resulted in no reaction or only trace to low yields. Collectively, these results underscore the uniquely effective role of MnO_2 in combination with $PdCl_2$, highlighting the superior catalytic performance of the $PdCl_2$/PivOH/MnO_2 system in promoting the present C–H activation and diarylation process.

Next, we investigated the substrate scope of various 2-alkynyl indoles bearing different functional groups using the optimized catalytic system (Table 2). Notably, the TFA additive showed a prominent effect on the reaction efficiency. For example, 2-alkynyl indoles with a phenyl group or a strongly electron-donating 4-methoxyphenyl group on the N-atom afforded the corresponding products **2b** and **2c** only in moderate yields in the absence of TFA, likely due to partial decomposition of the indole substrates. In contrast, the addition of 10 mol% TFA significantly improved the efficiency, affording **2b** and **2c** in 90% and 72% yields, respectively. This beneficial effect of TFA was even more evident for indole substrates bearing electron-withdrawing groups. For instance, substrates with CF_3 or Cl substituents at the *para*-position of the *N*-phenyl ring gave poor yields without TFA, whereas the addition of TFA dramatically enhanced the efficiency, affording **2d** and **2e** in good to high yields. Likewise, the substrate bearing an electron-withdrawing CN group at the 3-position of the indole ring and an electron-donating *p*-tolyl group on the N-atom exhibited an outstanding TFA effect, delivering

Table 2 Substrate scope for the synthesis of **2**[a]

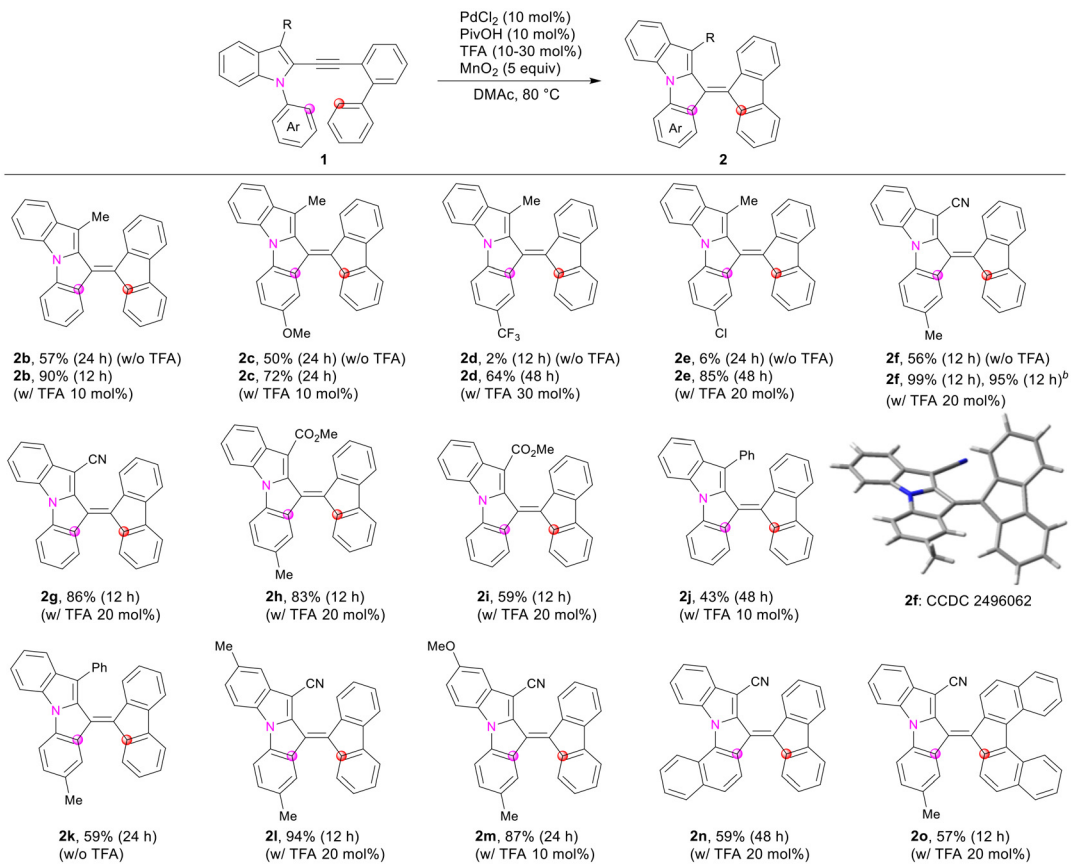

[a] Conditions: **1** (0.1 mmol), Pd (10 mol%), PivOH (10 mol%), TFA (10–30 mol%), and MnO_2 (5 equiv.) in DMAc (0.125 M, 0.8 mL) at 80 °C. Isolated yields of **2** after silica gel chromatography are shown. [b] The yield for the gram-scale synthesis of **2f** is shown.

2f in 99% yield. Notably, the gram-scale synthesis of **2f** also proceeded efficiently without obvious decrease in the isolated yield. The BPAE structure of **2f** was unambiguously confirmed by X-ray crystallographic analysis. As expected, the molecule exhibited a highly twisted geometry, with a dihedral angle of approximately 30° between the two polyaromatic rings, despite their connection through a C=C double bond. Furthermore, diarylation of indole substrates bearing electron-withdrawing CN or CO_2Me substituents at the 3-position of the indole ring in the presence of TFA produced the corresponding products **2g–i** in moderate to high yields. In contrast, substrates with a phenyl substituent at the 3-position of the indole ring afforded products **2j** and **2k** only in moderate yields, regardless of TFA, likely due to competitive diarylation between the 3-phenyl and biphenyl groups. The reaction was also compatible with substrates bearing CH_3 or OCH_3 substituents at the 5-position of the indole ring, affording **2l** and **2m** in 94% and 87% yields, respectively. Gratifyingly, the [5]helicene-conjugated BPAEs **2n** and **2o** were successfully synthesized *via* the diarylation of the corresponding *N*-naphthyl- or binaphthyl-alkyne-substituted indole substrates. In contrast, the substrate lacking a substituent at the 3-position of the indole ring failed to deliver the desired product, presumably because the high nucleophilicity at C3 promotes unproductive side reactions, leading to substrate decomposition.

Two intermolecular competitive kinetic isotope effect (KIE) experiments were carried out to probe the dual C–H activation process (Scheme S1 in the SI). In the reaction of a 1 : 1 mixture of **1f** and **1f-*d*$_7$**, where the deuterium atoms were incorporated on the *N*-*p*-tolyl group of the latter, a low KIE value of 1.0 was obtained under the standard conditions, both in the presence and absence of TFA (Scheme 2a). Similarly, the reaction of a 1 : 1 mixture of **1f** and **1f-*d*$_5$**, bearing deuterium atoms on the biphenyl moiety of the latter, gave slightly higher KIE values of 1.4 and 1.3, affording **2f-*d*$_4$** as an equimolar mixture of *syn*- and *anti*-diarylation products (Scheme 2b). These consistently low KIE values suggest that neither of the two C–H activation steps is likely to be rate-determining.

The most plausible reaction pathway (Path A), together with alternative pathways B and C, is illustrated in Scheme 2c and d. To gain deeper mechanistic insight into this transformation, density functional theory (DFT) calculations were performed at the M06/def2-SVP level for the reaction of **1b** in order to identify energetically favorable pathways, including key intermediates (IMs) and transition states (TSs) (Scheme 2d and e). The observation that a 1 : 1 $PdCl_2$: PivOH ratio gives the best activity, together with the poor catalytic performance of $Pd(OPiv)_2$ and $Pd(TFA)_2$ (Table 1), indicates that the catalytically active species is generated *in situ*. We therefore propose that the first step is ligand exchange between $PdCl_2$ and PivOH to afford a Cl–Pd–OPiv complex, with concurrent loss of HCl (Scheme 2c). This active Pd(II) species can coordinate to the alkyne moiety of **1b**, affording the π-complex **IM1A** (Path A). Subsequently, a pivalate-assisted C–H palladation occurs at the 2′-position of the biphenyl unit in **IM1A** through a concerted metallation–deprotonation (CMD) mechanism, leading to the formation of aryl–Pd complex **IM2A** *via* transition state **TS$_{1-2}$A** (Scheme 2c and e). Alternatively, a competing pathway (Path B), involving C–H palladation at the *ortho*-position of the *N*-phenyl ring in Pd-complex **IM1B**, was also considered (Scheme 2d, see Fig. S1 in SI). However, the calculated Gibbs free energy (ΔG) for **TS$_{1-2}$B** (+8.0 kcal mol^{-1}) is higher than that of **TS$_{1-2}$A** (+5.6 kcal mol^{-1}). Furthermore, the activation free energy ($\Delta G^{\ddagger}$) for **TS$_{1-2}$A** (+5.6 kcal mol^{-1}) is lower than that for **TS$_{1-2}$B** (+6.5 kcal mol^{-1}). These results clearly indicate that the initial C–H palladation at the biphenyl unit (*via* **TS$_{1-2}$A**) is both kinetically and thermodynamically more favorable than the corresponding process at the *N*-phenyl ring (*via* **TS$_{1-2}$B**), thereby validating Path A as the dominant pathway. Elimination of HCl from **IM2A** furnishes intermediate **IM3A**, which subsequently undergoes an intramolecular *syn*-insertion of the Pd–aryl bond into the alkyne through transition state **TS$_{3-4}$A** with a relatively high activation free energy ($\Delta G^{\ddagger}$ = 14.8 kcal mol^{-1}). This step affords the thermodynamically stable vinylpalladium complex **IM4aA**. An alternative pathway (Path C), previously proposed by our group,[22] involves CMD-type C–H activation of **IM3C** to generate a biaryl–Pd intermediate **IM4C** *via* **TS$_{3-4}$C**, followed by alkyne insertion (Scheme 2d). DFT calculations reveal that this pathway is both kinetically and thermodynamically unfavorable, as indicated by the high activation free energy of **TS$_{3-4}$C** ($\Delta G^{\ddagger}$ = 16.3 kcal mol^{-1}) and the low stability of **IM4C**. Conformational rotation of the *N*-phenyl ring converts **IM4aA** into **IM4bA**, which then undergoes a second, rapid pivalate-assisted CMD C–H activation at the *ortho*-position of the *N*-phenyl ring *via* **TS$_{4-5}$A** with a low $\Delta G^{\ddagger}$ of 2.1 kcal mol^{-1}, generating the six-membered palladacyclic intermediate **IM5A**. Subsequent elimination of PivOH from **IM5A** yields intermediate **IM6A**, which undergoes reductive elimination *via* **TS$_{6-7}$A** with a moderate activation barrier ($\Delta G^{\ddagger}$ = 9.2 kcal mol^{-1}), delivering **IM7A**. Decoordination of **IM7A** furnishes the final product **2b** together with a Pd(0) species. It is well established that MnO_2 reacts with HCl to generate Cl_2, $MnCl_2$, and H_2O. $PdCl_2$ can be formed by oxidation of Pd(0) with Cl_2 in the presence of HCl.[40] On this basis, we propose that the Pd(0) species generated in the final step is reoxidized to $PdCl_2$ by the *in situ*–generated Cl_2 under acidic conditions, thereby regenerating the active Pd(II) catalyst and completing the catalytic cycle (Scheme 2c). Additionally, for unsymmetrical products such as **2f-*d*$_4$** (Scheme 2b), the proposed *syn*-insertion mechanism predicts preferential formation of the *syn*-isomer. Partial post-reaction isomerization to the *anti*-isomer can nevertheless occur, resulting in a mixture of *syn*- and *anti*-diarylation products, consistent with observations reported in our previous study.[22]

Among the calculated steps, the *syn*-insertion process *via* **TS$_{3-4}$A** exhibits the highest activation barrier, identifying it as the rate-determining step of the catalytic cycle. To further elucidate the role of TFA as an additive, additional DFT calculations were performed on the corresponding trifluoroacetate-bound Pd species (Scheme 2e). The calculated ΔG for the TFA-bound intermediates and transition state, **IM3A′** (−4.6 kcal mol^{-1}), **TS$_{3-4}$A′** (+7.4 kcal mol^{-1}), and **IM4aA′** (−25.0 kcal

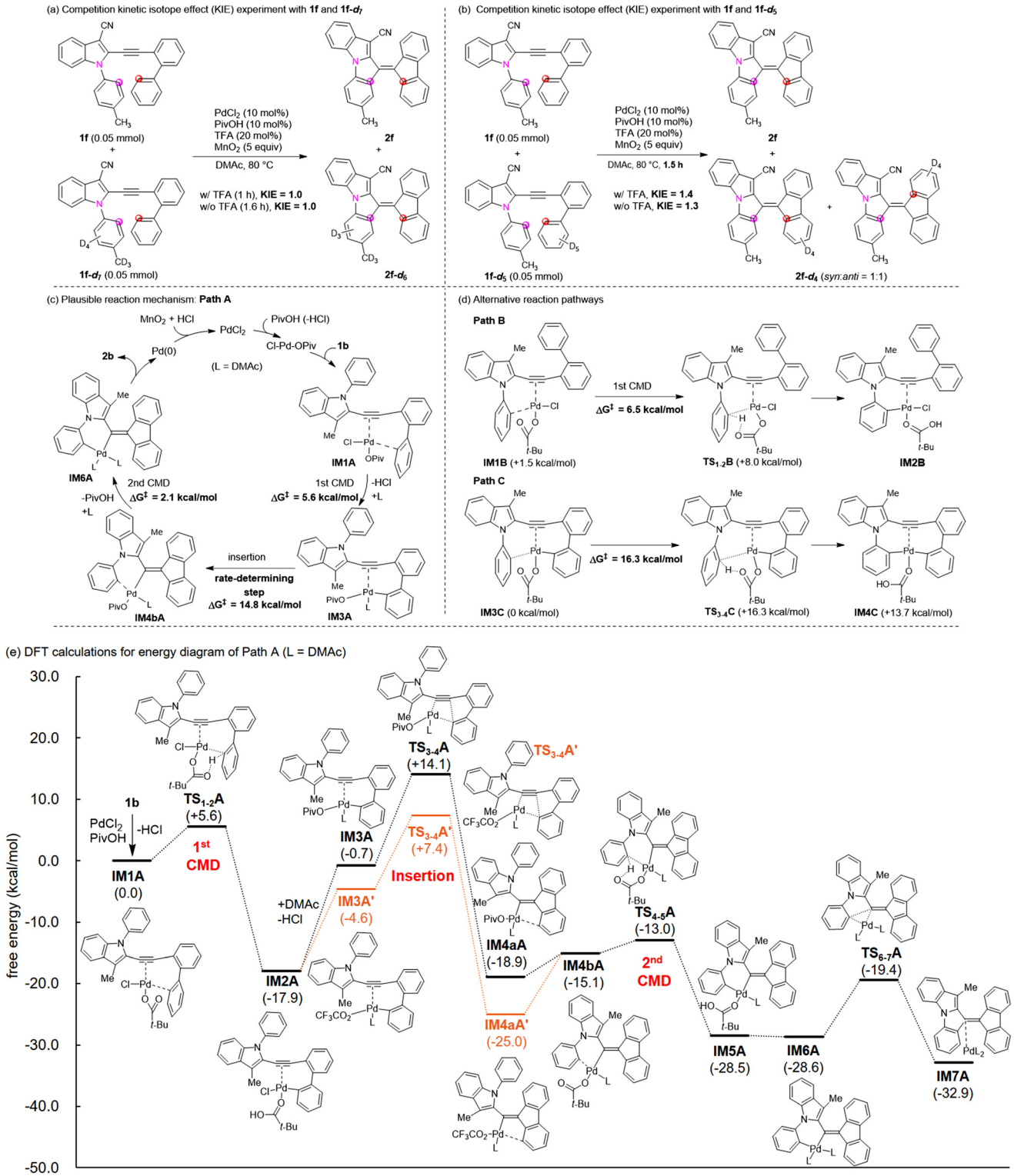

Scheme 2 Kinetic isotope effect (KIE) experiments and plausible reaction mechanism with energy diagram. KIE values were determined based on the product yields measured by ^{1}H NMR spectroscopy, using CH_2Br_2 as an internal standard. DFT computations were performed at the M06/def2-SVP level.

Table 3 Substrate scope for the synthesis of **4**[a]

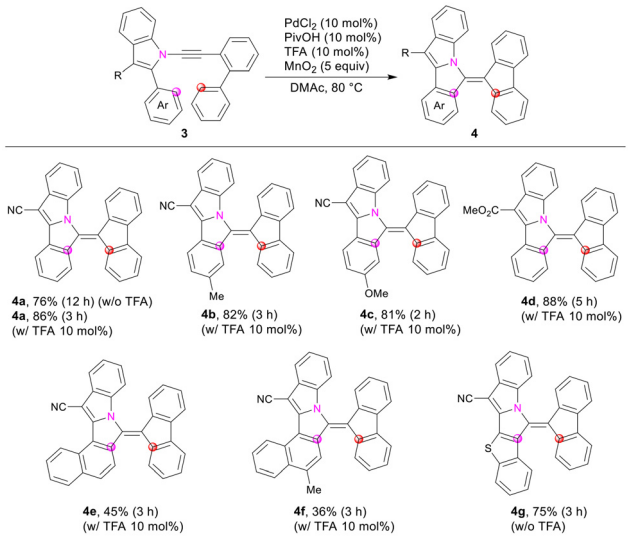

[a] Conditions: **3** (0.1 mmol), Pd (10 mol%), PivOH (10 mol%), TFA (10 mol%), and MnO_2 (5 equiv.) in DMAc (0.125 M, 0.8 mL) at 80 °C. Isolated yields of **4** after silica gel chromatography are shown.

mol^{-1}), are all markedly lower than those of the corresponding pivalate-bound species (**IM3A**, −0.7 kcal mol^{-1}; **TS$_{3-4}$A**, +14.1 kcal mol^{-1}; **IM4aA**, −18.9 kcal mol^{-1}). Notably, the $\Delta G^{\ddagger}$ of **TS$_{3-4}$A′** is 2.8 kcal mol^{-1} lower than that of **TS$_{3-4}$A**, indicating that coordination of TFA to the Pd center significantly stabilizes both the intermediate and transition-state species. These results suggest that TFA facilitates the *syn*-insertion step by lowering the associated energy barrier, thereby enhancing the overall reaction efficiency.

Encouraged by the successful diarylation method for constructing azafulvalene-based BPAEs, we next explored the synthesis of BPAEs incorporating positionally distinct azafulvalene cores. To this end, indole substrates **3**, bearing *N*-alkynyl biphenyl and 2-aryl substituents, were designed to afford the corresponding azafulvalene-based BPAEs **4** (Table 3). Electron-withdrawing substituents such as CN or CO_2Me were introduced at the 3-position of the indole ring to enhance the stability of the *N*-alkynyl moiety. Optimization studies revealed that the addition of TFA as an additive in the $PdCl_2$/PivOH/MnO_2 catalytic system significantly improved the reaction efficiency. For instance, the inclusion of 10 mol% TFA furnished product **4a** in 86% yield within 3 h, whereas only 76% yield was obtained after 12 h in the absence of TFA. Indoles bearing electron-donating Me or MeO substituents at the *para*-position

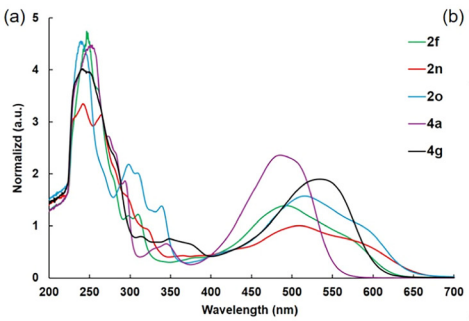

(b)

Compd.	λ_{max} (nm)[a]	λ_{onset} (nm)[a]	$HOMO_{exp}$ (eV)[b]	$LUMO_{exp}$ (eV)[b]	ΔE_{exp} (eV)[c]
99'BF	458.0	513.0	-5.58	-3.37	2.42[f]
			-5.34[d]	-2.51[d]	-2.83[d]
2f	575.0	623.0	-5.46	-3.47[e]	1.99[f]
2n	582.5	656.5	-5.40	-3.51[e]	1.89[f]
2o	585.5	643.0	-5.44	-3.51	1.93
4a	498.5	551.0	-5.53	-3.63	1.90
4g	534.0	603.5	-5.49	-3.62	1.87

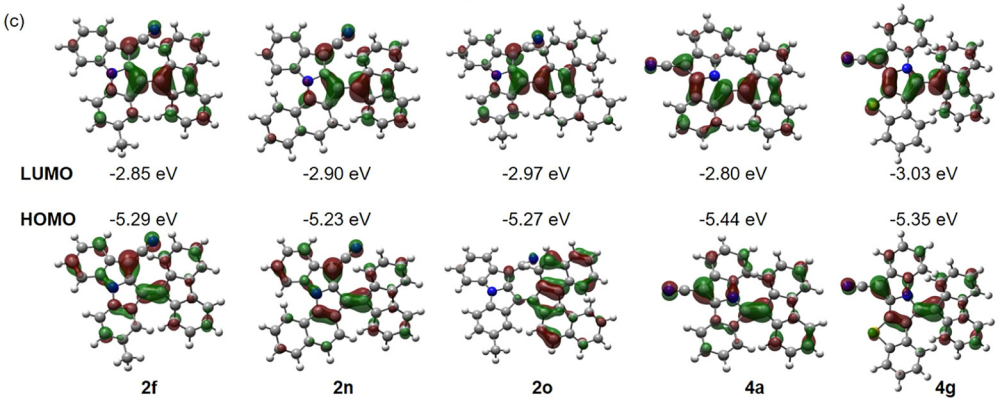

Fig. 1 (a) UV/Vis absorption spectra of selected BPAEs **2** and **4** in $CHCl_3$ (10^{-4} M). (b) Optical and electrochemical properties of BPAEs. [a] λ_{max} and λ_{onset} estimated from the maximum absorption at the longest wavelength and absorption onsets, respectively. [b] HOMO and LUMO was calculated from the oxidation and reduction potentials by CV measurement and the Fc/Fc+ (−4.80 eV) was used as an external standard. [c] HOMO–LUMO energy gap (ΔE_{exp}) was calculated from the HOMO and LUMO energy levels by CV measurement. [d] HOMO and LUMO energies, and energy gap of **99'BF** were calculated by DFT computations at the B3LYP/6-31G(d,p) level. [e] The LUMO energy was calculated from the HOMO energy and the optical energy gap (ΔE_{exp}). [f] Optical energy gap (ΔE_{exp}) was estimated from the onsets of UV/Vis absorbance (λ_{onset}). (c) DFT computations of HOMO and LUMO contours, and energy levels of BPAEs were carried out at the B3LYP/6-31G(d,p) level.

of the 2-phenyl ring exhibited negligible electronic effects, affording the corresponding products **4b** and **4c** in similarly high yields. Replacing the CN group with a CO_2Me substituent at the 3-position of the indole ring had little influence on the reactivity, and product **4d** was obtained in high yield. Furthermore, activation of the aromatic C–H bond at the 2-position of the naphthyl group on the indole ring proceeded smoothly, producing the π-extended BPAEs **4e** and **4f** in moderate yields. Notably, an *N*-alkynyl indole bearing a 2-benzothienyl substituent was also compatible with the current catalytic system, delivering the linear heteroacene-conjugated product **4g** in 75% yield, regardless of the presence or absence of TFA.

The UV/Vis absorption spectra of selected newly synthesized BPAEs in dilute chloroform are shown in Fig. 1a, and the corresponding longest absorption maxima (λ_{max}) and absorption onsets (λ_{onset}) are summarized in Fig. 1b. The azafulvalene-based BPAEs exhibit broad absorption bands extending to 550–650 nm, with both λ_{max} and λ_{onset} significantly red-shifted compared to the fulvalene-based analogue 99′BF.[1] Notably, compounds **2f**, **2n**, and **2o**, which possess an N-atom positioned away from the olefin bridge, display further bathochromic shifts compared to **4a** and **4g** containing an enamine motif. The frontier molecular orbital energy levels were estimated from cyclic voltammetry measurements (Fig. 1b). The new BPAEs exhibit slightly higher-lying HOMO levels (−5.40 to −5.53 eV) and markedly lower-lying LUMO levels (−3.47 to −3.63 eV) than those of 99′BF (HOMO: −5.58 eV; LUMO: −3.37 eV),[1] resulting in narrower HOMO–LUMO gaps and consequently longer wavelength absorptions. These experimental observations are consistent with the results of density functional theory (DFT) calculations performed at the B3LYP/6-31G(d,p) level (Fig. 1c). DFT-based orbital contour analyses indicate that the HOMOs of **2f**, **2n**, **4a**, and **4g** are delocalized from the N-atom-containing polyaromatic ring to the olefin bridge, whereas their LUMOs are predominantly localized on the azafulvalene core, excluding the N-atom. In contrast, the HOMO of **2o** is primarily localized on the helical polyaromatic segment, while its LUMO resides on the azafulvalene core. These distributions suggest a donor–acceptor type electronic structure that facilitates intramolecular charge transfer upon excitation. Time-dependent DFT (TD-DFT) calculations at the CAM-B3LYP/6-311+G(2d,p) level further indicate that, for compounds **2f**, **2n**, **4a**, and **4g**, the lowest singlet excited state (S_1) arises predominantly from a HOMO → LUMO transition (see Tables S1–S5, SI). In contrast, compound **2o** exhibits a dark S_1 state with negligible oscillator strength corresponding to a HOMO−1 → LUMO transition, while its bright S_2 state mainly involves the HOMO → LUMO transition.

Conclusions

We have developed an efficient Pd(II)-catalyzed intramolecular diarylation of alkynes that enables the selective synthesis of previously inaccessible azafulvalene-based bis(polycyclic) aromatic enes (BPAEs) through dual C–H bond activation. This method allows precise incorporation of nitrogen atoms into π-extended frameworks, offering modular access to structurally diverse BPAEs. Mechanistic and DFT studies revealed that the reaction proceeds *via* a pivalate-assisted CMD pathway, with the syn-insertion step identified as rate-determining. The additive effect of TFA was found to lower the energy barrier of this key step, thereby enhancing overall efficiency. The resulting azafulvalene-based BPAEs exhibit narrow HOMO–LUMO gaps, red-shifted absorption extending into the visible region, and low-lying LUMO levels, consistent with donor–acceptor type electronic structures predicted by DFT and TD-DFT calculations. These findings demonstrate a powerful strategy for constructing π-extended nitrogen-containing fulvalene architectures and highlight the potential of azafulvalene-based BPAEs as promising building blocks for future organic optoelectronic materials.

Author contributions

T. J. and M. T. conceived and designed the project and wrote the manuscript with the assistance of other authors. S. A. conducted experiments. T. S. performed theoretical calculations. All the authors analyzed the data and discussed the results.

Conflicts of interest

There are no conflicts to declare.

Data availability

Supplementary information (SI): experimental procedures, computational data, and characterization of related compounds. See DOI: **https://doi.org/10.1039/d5qo01688f**.

CCDC 2496062 contains the supplementary crystallographic data for this paper.[41]

Acknowledgements

This research was supported by a Grant-in-Aid for Transformative Research Areas (A) "Green Catalysis Science for Renovating Transformation of Carbon-Based Resources" (JP23H04908) from MEXT, Japan and a Grant-in-Aid for Scientific Research (S) (JP22H04969) from the JSPS. The computation was performed using Research Center for Computational Science, Okazaki, Japan (Project: 25-IMS-C110).

References

1 F. G. Brunetti, X. Gong, M. Tong, A. J. Heeger and F. Wudl, Strain and Hückel Aromaticity: Driving Forces for a Promising New Generation of Electron Acceptors in

Organic Electronics, *Angew. Chem., Int. Ed.*, 2010, **49**, 532–536.
2 C.-Y. Chiu, H. Wang, F. G. Brunetti, F. Wudl and C. J. Hawker, Twisted but Conjugated: Building Blocks for Low Bandgap Polymers, *Angew. Chem., Int. Ed.*, 2014, **53**, 3996–4000.
3 K. Rakstys, M. Saliba, P. Gao, P. Gratia, E. Kamarauskas, S. Paek, V. Jankauskas and M. K. Nazeeruddin, Highly Efficient Perovskite Solar Cells Employing an Easily Attainable Bifluorenylidene-Based Hole-Transporting Material, *Angew. Chem., Int. Ed.*, 2016, **55**, 7464–7468.
4 X. Lai, M. Du, F. Meng, G. Li, W. Li, A. K. K. Kyaw, Y. Wen, C. Liu, H. Ma, R. Zhang, D. Fan, X. Guo, Y. Wang, H. Ji, K. Wang, X. W. Sun, J. Wang and W. Huang, High-Performance Inverted Planar Perovskite Solar Cells Enhanced by Thickness Tuning of New Dopant-Free Hole Transporting Layer, *Small*, 2019, **15**, 1904715.
5 H.-W. Kang, Y.-C. Liu, W.-K. Shao, Y.-C. Wei, C.-T. Hsieh, B.-H. Chen, C.-H. Lu, S.-D. Yang, M.-J. Cheng, P.-T. Chou, M.-H. Chiang and Y.-T. Wu, Synthesis, structural analysis, and properties of highly twisted alkenes 13,13′-bis(dibenzo[*a*,*i*]fluorenylidene) and its derivatives, *Nat. Commun.*, 2023, **14**, 5248.
6 B. Prajapati, M. D. Ambhore, D.-K. Dang, P. J. Chmielewski, T. Lis, C. J. Gomez-Garcia, P. M. Zimmerman and M. Stępień, Tetrafluorenofulvalene as a sterically frustrated open-shell alkene, *Nat. Chem.*, 2023, **15**, 1541–1548.
7 B. L. Feringa, W. F. Jager, B. de Lange and E. W. Meijer, Chiroptical molecular switch, *J. Am. Chem. Soc.*, 1991, **113**, 5468–5470.
8 N. P. M. Huck, W. F. Jager, B. de Lange and B. L. Feringa, Dynamic Control and Amplification of Molecular Chirality by Circular Polarized Light, *Science*, 1996, **273**, 1686–1688.
9 B. L. Feringa, In Control of Motion: From Molecular Switches to Molecular Motors, *Acc. Chem. Res.*, 2001, **34**, 504–513.
10 J. Vicario, M. Walko, A. Meetsma and B. L. Feringa, Fine Tuning of the Rotary Motion by Structural Modification in Light-Driven Unidirectional Molecular Motors, *J. Am. Chem. Soc.*, 2006, **128**, 5127–5135.
11 D. J. van Dijken, P. Štacko, M. C. A. Stuart, W. R. Browne and B. L. Feringa, Chirality controlled responsive self-assembled nanotubes in water, *Chem. Sci.*, 2017, **8**, 1783–1789.
12 M. B. S. Wonink, B. P. Corbet, A. A. Kulago, G. B. Boursalian, B. de Bruin, E. Otten, W. R. Browne and B. L. Feringa, Three-State Switching of an Anthracene Extended Bis-thiaxanthylidene with a Highly Stable Diradical State, *J. Am. Chem. Soc.*, 2021, **143**, 18020–18028.
13 E. M. Pérez, M. Sierra, L. Sánchez, M. R. Torres, R. Viruela, P. M. Viruela, E. Ortí and N. Martín, Concave Tetrathiafulvalene-Type Donors as Supramolecular Partners for Fullerenes, *Angew. Chem., Int. Ed.*, 2007, **46**, 1847–1851.
14 H. Xue, C. Ye, H. Huang and H. Bao, Steric Gating of Excited-State Channel: Controllable AIE/RTP Switching through Tuning π-Bond Twisting, *Org. Lett.*, 2025, **27**, 6163–6169.
15 P. U. Biedermann, J. J. Stezowski and I. Agranat, Polymorphism Versus Thermochromism: Interrelation of Color and Conformation in Overcrowded Bistricyclic Aromatic Enes, *Chem. – Eur. J.*, 2006, **12**, 3345–3354.
16 T. Suzuki, H. Okada, T. Nakagawa, K. Komatsu, C. Fujimoto, H. Kagi and Y. Matsuo, A fluorenylidene-acridane that becomes dark in color upon grinding–ground state mechanochromism by conformational change, *Chem. Sci.*, 2018, **9**, 475–482.
17 Y. Matsuo, Y. Wang, H. Ueno, T. Nakagawa and H. Okada, Mechanochromism, Twisted/Folded Structure Determination, and Derivatization of (*N*-Phenylfluorenylidene)acridane, *Angew. Chem., Int. Ed.*, 2019, **58**, 8762–8767.
18 M. Shimizu, K. Nishimura, M. Mineyama, R. Terao, T. Sakurai and H. Sakaguchi, Bis(tricyclic) Aromatic Enes That Exhibit Efficient Fluorescence in the Solid State, *Molecules*, 2024, **29**, 5361.
19 M. N. Tran and D. M. Chenoweth, Photoelectrocyclization as an Activation Mechanism for Organelle-Specific Live-Cell Imaging Probes, *Angew. Chem., Int. Ed.*, 2015, **54**, 6442–6446.
20 Y. Ishigaki, Y. Hayashi and T. Suzuki, Photo- and Thermal Interconversion of Multiconfigurational Strained Hydrocarbons Exhibiting Completely Switchable Oxidation to Stable Dicationic Dyes, *J. Am. Chem. Soc.*, 2019, **141**, 18293–18300.
21 M. Shimizu, I. Nagao, S.-i. Kiyomoto and T. Hiyama, New Synthesis of Dibenzofulvenes by Palladium-Catalyzed Double Cross-Coupling Reactions, *Aust. J. Chem.*, 2012, **65**, 1277–1284.
22 J. Zhao, N. Asao, Y. Yamamoto and T. Jin, Pd-Catalyzed Synthesis of 9,9′-Bifluorenylidene Derivatives via Dual C–H Activation of Bis-biaryl Alkynes, *J. Am. Chem. Soc.*, 2014, **136**, 9540–9543.
23 M. Zhang, W. Deng, M. Sun, L. Zhou, G. Deng, Y. Liang and Y. Yang, α-Bromoacrylic Acids as C1 Insertion Units for Palladium-Catalyzed Decarboxylative Synthesis of Diverse Dibenzofulvenes, *Org. Lett.*, 2021, **23**, 5744–5749.
24 S. Yang and Y. Zhang, Synthesis of 9-Fluorenylidenes via Pd-Catalyzed C–H Vinylation with Vinyl Bromides, *Org. Lett.*, 2021, **23**, 7746–7750.
25 X. Zhu, F. Liu, X. Ba and Y. Wu, Synthesis of Fused-Ring Derivatives Containing Bifluorenylidene Units via Pd-Catalyzed Tandem Multistep Suzuki Coupling/Heck Cyclization Reaction, *J. Org. Chem.*, 2023, **88**, 15964–15968.
26 M. Gao, X. Cui, L. Yang, H. Zhao and Y. Wu, Synthesis of Regular Ladder-Type Fluorenylidene-Xanthene Oligomers via Nucleophilic Aromatic Substitution Reaction, *Org. Lett.*, 2024, **26**, 9937–9942.
27 J. Corpas, P. Mauleón, R. G. Arrayás and J. C. Carretero, Transition-Metal-Catalyzed Functionalization of Alkynes with Organoboron Reagents: New Trends, Mechanistic

Insights, and Applications, *ACS Catal.*, 2021, **11**, 7513–7551.

28 H. Oda, M. Morishita, K. Fukami, H. Sano and M. Kosugi, A Novel Diarylation Reaction of Alkynes by Using Aryltributylstannane in the Presence of Palladium Catalyst, *Chem. Lett.*, 1996, **25**, 811–812.

29 C. Zhou, D. E. Emrich and R. C. Larock, An Efficient, Regio- and Stereoselective Palladium-Catalyzed Route to Tetrasubstituted Olefins, *Org. Lett.*, 2003, **5**, 1579–1582.

30 F. Xue, J. Zhao, T. S. A. Hor and T. Hayashi, Nickel-Catalyzed Three-Component Domino Reactions of Aryl Grignard Reagents, Alkynes, and Aryl Halides Producing Tetrasubstituted Alkenes, *J. Am. Chem. Soc.*, 2015, **137**, 3189–3192.

31 W. Lv, S. Liu, Y. Chen, S. Wen, Y. Lan and G. Cheng, Palladium-Catalyzed Intermolecular Trans-Selective Carbofunctionalization of Internal Alkynes to Highly Functionalized Alkenes, *ACS Catal.*, 2020, **10**, 10516–10522.

32 S. Dutta, S. Shandilya, S. Yang, M. P. Gogoi, V. Gandon and A. K. Sahoo, Cationic-palladium catalyzed regio- and stereoselective *syn*-1,2-dicarbofunctionalization of unsymmetrical internal alkynes, *Nat. Commun.*, 2022, **13**, 1360.

33 S. P. Sancheti, Y. Singh, M. V. Mane and N. T. Patil, Gold-Catalyzed 1,2-Dicarbofunctionalization of Alkynes with Organohalides, *Angew. Chem., Int. Ed.*, 2023, **62**, e202310493.

34 B. Milde, A. Reding, F. J. Geffers, P. G. Jones and D. B. Werz, Intramolecular *trans*-Dicarbofunctionalization of Alkynes by a Formal *anti*-Carbopalladation/Stille Cascade, *Chem. – Eur. J.*, 2016, **22**, 14544–14547.

35 A. Reding, P. G. Jones and D. B. Werz, *trans*-Carbocarbonation of Internal Alkynes through a Formal *anti*-Carbopalladation/C–H Activation Cascade, *Angew. Chem., Int. Ed.*, 2018, **57**, 10610–10614.

36 L. F. Tietze, T. Hungerland, C. Depken, C. Maaß and D. Stalke, Palladium-Catalyzed Domino Carbopalladation/C–H Activation for the Synthesis of Tetrasubstituted Alkenes Bearing Five- and Seven-Membered Rings, *Synlett*, 2012, 2516–2520.

37 L. F. Tietze, T. Hungerland, A. Düfert, I. Objartel and D. Stalke, Synthesis of Tetrasubstituted Alkenes through a Palladium-Catalyzed Domino Carbopalladation/C–H-Activation Reaction, *Chem. – Eur. J.*, 2012, **18**, 3286–3291.

38 L. F. Tietze, T. Hungerland, C. Eichhorst, A. Düfert, C. Maaß and D. Stalke, Efficient Synthesis of Helical Tetrasubstituted Alkenes as Potential Molecular Switches: A Two-Component Palladium-Catalyzed Triple Domino Process, *Angew. Chem., Int. Ed.*, 2013, **52**, 3668–3671.

39 L. F. Tietze, B. Waldecker, D. Ganapathy, C. Eichhorst, T. Lenzer, K. Oum, S. O. Reichmann and D. Stalke, Four- and Sixfold Tandem-Domino Reactions Leading to Dimeric Tetrasubstituted Alkenes Suitable as Molecular Switches., *Angew. Chem., Int. Ed.*, 2015, **54**, 10317–10321.

40 *Handbook of Preparative Inorganic Chemistry*, ed. G. Brauer, Academic Press, New York, London, 1963.

41 CCDC 2496062: Experimental Crystal Structure Determination, 2026, DOI: **10.5517/ccdc.csd.cc2psc40**.